ISSN 1738-6055 (Print)
ISSN 2233-7660 (Online)

Lab Anim Res 2016: 32(1), 1-7
http://dx.doi.org/10.5625/lar.2016.32.1.1

Laboratory Animal Research
http://submission.kalas.or.kr

Postnatal changes in glucose transporter 3 expression in the dentate gyrus of the C57BL/6 mouse model

Hyo Young Jung[1], Hee Sun Yim[2], Dae Young Yoo[1], Jong Whi Kim[1], Jin Young Chung[3], Je Kyung Seong[1,4], Yeo Sung Yoon[1,4], Dae Won Kim[2], In Koo Hwang[1,4,*]

[1]*Department of Anatomy and Cell Biology, College of Veterinary Medicine, and Research Institute for Veterinary Science, Seoul National University, Seoul 08826, Korea*

[2]*Department of Biochemistry and Molecular Biology, Research Institute of Oral Sciences, College of Dentistry, Kangneung-Wonju National University, Gangneung 25457, Korea*

[3]*Department of Veterinary Internal Medicine and Geriatrics, College of Veterinary Medicine, Kangwon National University, Chuncheon 24341, Korea*

[4]*KMPC (Korea Mouse Phenotyping Center), Seoul National University, Seoul 08826, Korea*

In this study, we observed the ontogenetic changes in glucose transporter 3 (GLUT3) immunoreactivity, a major neuronal GLUT, in the dentate gyrus of mouse brains at various ages: postnatal day (P) 1, 7, 14, 28, and 56. At P1, cresyl violet staining showed abundant neurons in the dentate gyrus, whereas the granule cell layer was ill-defined. At P7, the granule cell layer was observed, and cresyl violet-positive cells were dispersed throughout the polymorphic layer. At P14, the granule cell layer was well-defined, and cresyl violet positive cells were detected abundantly in the polymorphic layer. At P28 and P56, cresyl violet-positive cells were observed in the granule cell layer, as well as in the polymorphic layer. At P1, GLUT3 immunoreactivity was detected in the dentate gyrus. At P7, GLUT3 immunoreactive cells were scattered in the polymorphic and molecular layer. However, at P14, GLUT3 immunoreactivity was observed in the polymorphic layer as well as subgranular zone of the dentate gyrus. At P28, GLUT3 immunoreactivity was detected in the polymorphic layer of the dentate gyrus. At P56, GLUT3 immunoreactivity was observed predominantly in the subgranular zone of the dentate gyrus. GLUT3 immunoreactive cells were mainly colocalized with doublecortin, which is a marker for differentiated neuroblasts, in the polymorphic layer and subgranular zone of dentate gyrus at P14 and P56. These results suggest that the expression of GLUT3 is closely associated with postnatal development of the dentate gyrus and adult neurogenesis.

Keywords: Dentate gyrus, glucose transporter 3, mice, neuroblast, postnatal development

Received 6 January 2016; Revised version received 17 February 2016; Accepted 3 March 2016

The hippocampus is one of the oldest systems in the cerebral cortex (archicortex), and is responsible for recent memory formation and limbic functions. In particular, the dentate gyrus consists of archicortical precursor cells in the developing mammalian embryo [1]. During embryogenesis, only 15% of granule cells are produced, and the remaining are produced during the first two weeks of postnatal development in the mouse [2,3]. Recently, the dentate gyrus has been focused upon because of its special ability to produce new neurons and glia throughout the entire lifetime [4,5].

The brain and spinal cord comprise about 2% of the body's total mass, but these organs utilize approximately 25% of the body's total glucose [6]. Glucose is the primary energy source in the brain, and more glucose is required during postnatal development and adult neuro-

*Corresponding author: In Koo Hwang, Department of Anatomy and Cell Biology, College of Veterinary Medicine, Seoul National University, Seoul 08826, Korea
Tel: +82-2-880-1271; E-mail: vetmed2@snu.ac.kr

genesis. The uptake and utilization of glucose across the cell membrane is facilitated by a family of integral membrane transporter proteins, glucose transporters (GLUTs) [7], with GLUT1 and GLUT3 being the most important glucose transporters in the brain [8]. GLUT1 is expressed in the microvascular endothelial cells and astrocytes and carries glucose across the blood-brain barrier. In contrast, GLUT3 is observed at the plasma membrane of neurons and is responsible for the uptake of glucose into neurons [8-10].

Several lines of evidence indicate that changes in GLUT3 expression show a strong correlation with rates of glucose utilization based on 2-deoxy[^{14}C]glucose uptake in postnatal rats [11,12]. However, there are few reports of changes in GLUT3 in the dentate gyrus after postnatal development. In this study, we investigated morphological changes in GLUT3 immunoreactivity in the dentate gyrus at various postnatal stages. In addition, we also observed the correlation of GLUT3 immunoreactive cells with neuroblasts in the dentate gyrus of postnatal mice.

Materials and Methods

Experimental animals

Our study used young [postnatal days (P): 1, 7, 14, 28, and 56, n=5 for each] male C57BL/6J mice. The day of birth was considered as day 0. Litters were culled to a maximum of 8 pups at the day of birth. From any one litter, a maximum two animals were taken for each age group, ensuring that animals of a given age originated from at least four different litters. The handling and care of the animals conformed to the guidelines established to comply with current international laws and policies (NIH Guide for the Care and Use of Laboratory Animals, NIH Publication No. 85-23, 1985, revised 1996), and were approved by the Institutional Animal Care and Use Committee (IACUC) of Seoul National University (Approval no.: SNU-140313-1). All of the experiments were conducted with an effort to minimize the number of animals used, and the suffering caused by the procedures employed in the present study.

Tissue processing and cresyl violet staining

Animals at each age were anesthetized by injecting urethane (1 g/kg body weight, i.p., Sigma, St. Louis, MO, USA) and the brain was removed. Thereafter, brain was fixed for 24 h in the 10% neutral buffered formalin at room temperature and dehydrated with graded concentrations of alcohol for embedding in paraffin. Thereafter, paraffin-embedded tissues were sectioned on a microtome (Leica, Wetzlar, Germany) into 3-μm coronal sections, and they were mounted into silane-coated slides. The sections were stained with cresyl violet staining according to the general protocol.

Immunohistochemistry for GLUT3

To ensure that the immunohistochemical data were comparable between groups, the sections were carefully processed under the same conditions. The sections were hydrated and treated with 0.3% hydrogen peroxide (H_2O_2) in PBS for 30 min. For antigen retrieval, the sections were placed in 400 mL jars filled with citrate buffer (pH 6.0) and heated in a microwave oven (Optiquick Compact, Moulinex, UK) operating at a frequency of 2.45 GHz and 800 W power setting. After three heating cycles of 5 min each, slides were allowed to cool at room temperature and were washed in PBS. After washing, the sections were incubated with 5% non-fat dry milk in PBS containing 0.1% Tween 20 for 45 min to reduce the background staining. Sections were incubated successively in 10% normal goat serum in PBS for 30 min, and in diluted rabbit anti-GLUT3 (diluted 1:50, SantaCruz Biotechnology, Santa Cruz, CA, USA) for 48 h at 4°C. Thereafter, they were exposed to biotinylated goat anti-rabbit IgG and streptavidin peroxidase complex (diluted 1:200, Vector, Burlingame, CA, USA) and visualized with 3,3'-diaminobenzidine tetrahydrochloride (Sigma) in 0.1 M Tris-HCl buffer (pH 7.4).

Double immunofluorescence staining of GLUT3 and doublecortin (DCX)

To confirm the colocalization of GLUT3 and DCX in the brain, the sections at P14 and P56 group were processed by double immunofluorescence staining under the same conditions. Double immunofluorescence staining for rabbit anti-GLUT3 (1:20)/goat anti-DCX (diluted 1:25; SantaCruz Biotechnology) was performed. The sections were incubated in the mixture of antisera overnight at room temperature. After washing 3 times for 10 min with PBS, they were then incubated in a mixture of both Cy3-conjugated donkey anti-rabbit IgG (1:600; Jackson ImmunoResearch, West Grove, PA, USA) and FITC-conjugated donkey anti-goat IgG (1:600; Jackson ImmunoResearch) for 2 h at room

temperature. The immunoreactions were observed under the BX51 microscope attached HBO100 (Olympus, Tokyo, Japan).

Data analysis

The measurement of GLUT3-positive cells in all the groups was performed using an image analysis system equipped with a computer-based CCD camera (software: Optimas 6.5, CyberMetrics, Scottsdale, AZ, USA) in a tissue area observed under 100× primary magnification. In brief, GLUT3-positive neurons were counted at the center of the dentate gyrus and the image was converted to a gray image and GLUT3-positive neurons were automatically selected according to the intensity of GLUT3 immunostaining. Cell counts were obtained for each animal by averaging the counts from 25 sections, and the cell number was reported as a percentage of that obtained from the P1 groups.

Analysis of the regions of interest in the dentate gyrus was performed using an image analysis system. GLUT3 immunoreactivity was evaluated by relative optical density (ROD), which was obtained after transformation of the mean gray level using the formula: ROD=log (256/mean gray level). ROD of background was determined in unlabeled portions and this value was subtracted for correction, yielding high ROD values in the presence of preserved structures and low values after structural loss using NIH Image 1.59 software (National Institutes of Health, Bethesda, MD, USA). A ratio of the ROD was calibrated as percentage compared to control. ROD was analyzed in 10 cells from 25 sections, and the immunoreactivity was reported as a percentage of that obtained from the P1 groups.

The data express the means of the experiments performed for each experimental investigation. The differences among the means were statistically analyzed using a one-way analysis of variance followed by Bonferroni's post-hoc test in order to compare the changes of GLUT3. Statistical significance was considered at $P<0.05$.

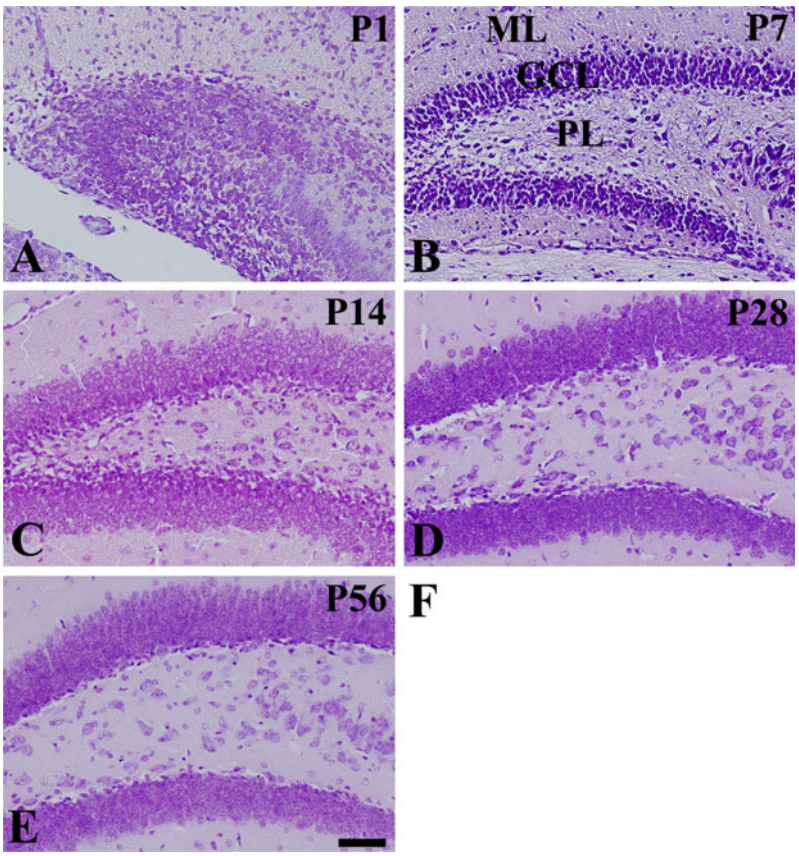

Figure 1. Cresyl violet staining in the mouse dentate gyrus at P1 (A), P7 (B), P14 (C), P28 (D), and P56 (E). Cresyl violet-positive neurons are dispersed throughout the dentate gyrus by P7. Cresyl violet-positive neurons are detected in the granule cell layer (GCL) and well-laminated into three layers at P14. ML, molecular layer; PL, polymorphic layer. Scale bar=50 μm.

Results

Cresyl violet staining

In the P1 group, cresyl violet staining showed neurons were detected in a diffuse pattern in the dentate gyrus in three layers: the granule cell layer, the molecular layer, and the polymorphic layer, although the polymorphic layer was ill-defined (Figure 1A). In the P7 group, the dentate gyrus also showed three layers, but cresyl violet-positive neurons were more abundant in the polymorphic layer and were dispersed throughout the polymorphic layer rather than granular cell layer (Figure 1B). In the

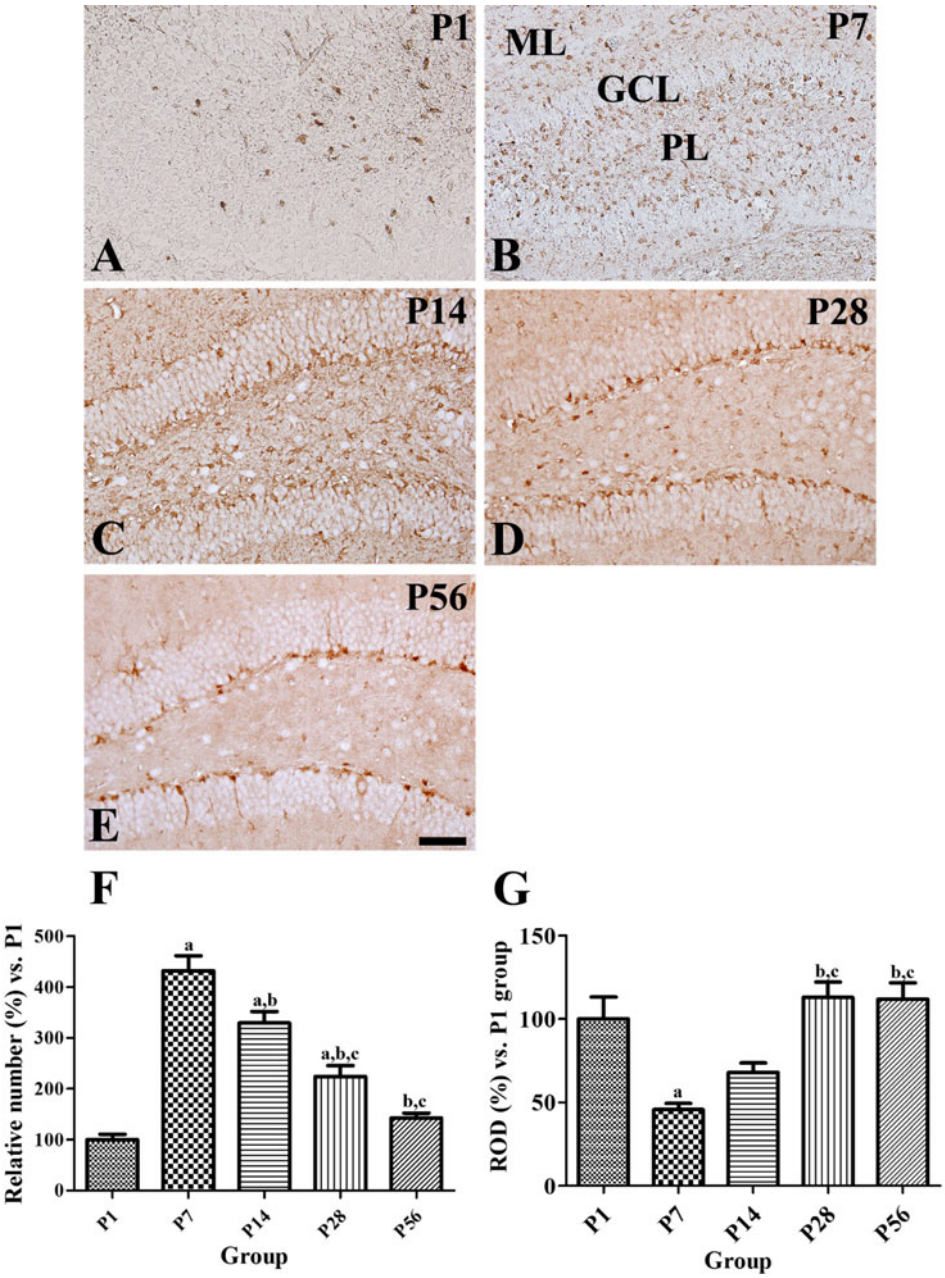

Figure 2. Immunohistochemical staining for glucose transporter 3 (GLUT3) in the mouse dentate gyrus at P1 (A), P7 (B), P14 (C), P28 (D), and P56 (E). GLUT3 immunoreactivity is detected in the cell body and neuropils of the polymorphic (PL) and granule cell layers (GCL) of the dentate gyrus at P14. In the P28 and P56 groups, GLUT3 immunoreactivity is mainly observed in the subgranular zone of the dentate gyrus. ML, molecular layer. Scale bar=50 μm. F and G: The number of GLUT3 immunoreactive cells and relative optical density (ROD) of GLUT3 immunoreactivity in the dentate gyrus at P1, P7, P14, P28, and P56 are expressed as percentage of P1 group (n=5 per group; $^{a}P<0.05$, significantly different from the P1 group; $^{b}P<0.05$, significantly different from the P7 group; $^{c}P<0.05$, significantly different from the P14 group; $^{d}P<0.05$, significantly different from the P28 group). All data are represented as the mean±standard errors of mean.

P14 group, cresyl violet-positive neurons were abundantly detected in the granule cell layer of the dentate gyrus, but the cresyl violet-positive neurons were decreased in the polymorphic layer (Figure 1C). In the P28 group, cresyl violet-positive neurons were more compact in the granule cell layer, and the number of cells was decreased in the polymorphic layer (Figure 1D). In the P28 and P56 groups, the distribution pattern of cresyl violet-positive neurons was similar within the dentate gyrus (Figure 1D and 1E).

GLUT3 immunoreactivity

In the P1 group, GLUT3 immunoreactivity was found in the polymorphic layer of dentate gyrus (Figure 2A). In the P7 groups, GLUT3 immunoreactivity was abundantly detected in the molecular and polymorphic layer of dentate gyrus (Fig. 2B). In the P14 group, GLUT3 immunoreactivity was observed in the polymorphic and molecular cell layers of the dentate gyrus in the cell body and neuropils (Figure 2C). In the P28 and P56 groups, GLUT3 immunoreactive structures were also detected in the neuronal processes, whereas GLUT3-immunoreactive neurons were located in the subgranular zone of the dentate gyrus (Figure 2D, 2E). In the P7, P14, P28, and P56 groups, the number of GLUT3-immunoreactive neurons decreased significantly with age (Figure 2F), while GLUT3 immunoreactivity was increased significantly with age (Figure 2G).

Co-localization of GLUT3 and DCX

In the P14 group, GLUT3- and DCX-labeled cells were detected abundantly in the polymorphic layer and middle line of the granule cell layer (Figure 3A-3C). In contrast, GLUT3- and DCX-labeled cells in the P56 group were confined to the subgranular zone of the dentate gyrus (Figure 3D-3F).

Discussion

Glucose is the main energy substrate for the brain, and GLUT is the most efficient GLUT isoform and plays a major role in fueling neuronal transmission [10]. In this study, we investigated the postnatal development of neurons and expression of GLUT3 in the dentate gyrus, because 80-90% of the granule cells in the dentate gyrus are formed postnatally, unlike other neuronal cells in the hippocampus [2,3,13,14]. The architecture of the dentate gyrus was nearly completely developed in the P14 group, as the three layers of the dentate gyrus were detected prominently. This result was supported by our previous study as well as other studies demonstrating that hippocampal development was complete at P14-P15 in mouse [15] and rat [16] models. However, some neurons at P14 were dispersed within the polymorphic layer of the dentate gyrus, and we found that GLUT3 was expressed in these neurons. In the P28 and P56 groups, GLUT3 immunoreactivity was mainly found in

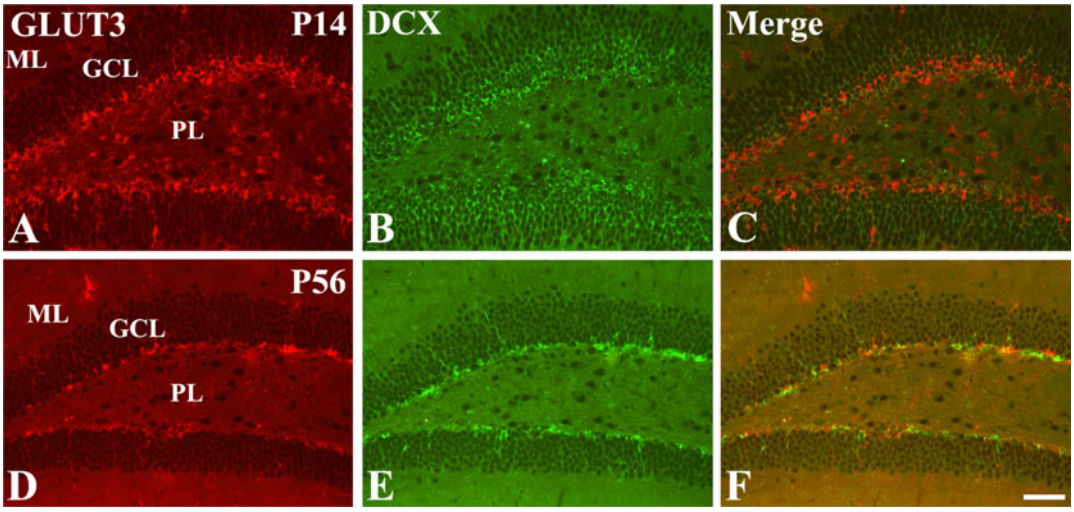

Figure 3. Immunofluorescence staining for GLUT3 (A and D, red), doublecortin (DCX, B and E, green), and merged images (C and F, yellow) in the dentate gyrus in the P14 and P56 groups. Note that GLUT3 and DCX double-labeled cells are abundant in the polymorphic layer of the dentate gyrus in the P14 group, while in the P56 group these cells are mainly detected in the subgranular zone of the dentate gyrus. Scale bar=50 μm.

the subgranular zone of the dentate gyrus, and these GLUT3 immunoreactive neurons were confirmed to be neuroblasts based on a double immunofluorescence study for GLUT3 and DCX. These results suggest that GLUT3 constitutes one mechanism of supplying glucose to the neuroblasts in the dentate gyrus. In addition, the expression of GLUT3 in the polymorphic layer of the dentate gyrus at P14 may indicate that cells in the polymorphic layer are immature, and that full development of the dentate gyrus was not complete at P14 in the mouse.

In this study, we observed an age-dependent decrease in the number of GLUT3 immunoreactive neurons in the dentate gyrus at P7-P56. The decrease of GLUT3 immunoreactive neurons may be associated with the reduction of neuroblast number in the dentate gyrus with age [15]. This result is contradictory with previous study that showed GLUT3 levels increase in a linear fashion between P1 and P21 [17]. Nehlig and colleagues demonstrated the steady increase of local glucose utilization in the hippocampus [11]. Moreover, synaptogenesis has been shown to increase rapidly in the cerebral cortex of rats between P10 and P26 [18]. However, in the present study, we observed a significant decrease in the number of GLUT3-immunoreactive neurons in the dentate gyrus at P28. Instead, the GLUT3 immunoreactivity was significantly increased in the dentate gyrus at P7-P28 and GLUT3 immunoreactivity was strongly detected in the cells located in the subgranular zone of the dentate gyrus at P28. This result suggests that GLUT3 may play a role in postnatal development of the hippocampus by P28, and thereafter has an important role in adult neurogenesis.

The phosphorylation of CREB (cAMP response element-binding protein) is implicated in both activity-dependent neuronal plasticity and neurotrophin-mediated neuronal survival [19,20]. CREB is one of the main transcription factors of the GLUT3 gene [15]. The phosphorylation of the CREB protein on serine 133 and the mouse Y box-binding protein could result in binding to the promoter region of GLUT3 and activate GLUT3 expression to mediate the energy demand in cells, including neurons [21-24]. In the previous study, we demonstrated that phosphorylated CREB on serine 133 (pCREB)-immunoreactive nuclei were detected strongly in the subgranular zone of the dentate gyrus at P21, and pCREB protein levels decreased with age, with very low levels observed at P21 [25]. The distribution pattern and immunoreactivity of pCREB correlated with that of GLUT3.

In conclusion, by P28 the location of GLUT3 immunoreactive neurons has changed from cells in the polymorphic and granule cell layers of the dentate gyrus to cells in the subgranular zone. In addition, GLUT3 immunoreactivity is detected in the DCX-positive neuroblasts in the dentate gyrus. These results suggest that the expression of GLUT3 is a very important factor in modulating the development of the dentate gyrus and adult neurogenesis, and full development of the dentate gyrus may be completed between P14 and P28.

Acknowledgments

This research was supported by Korea Mouse Phenotyping Project (2013M3A9D5072550) of the Ministry of Science, ICT and Future Planning through the National Research Foundation (NRF), Korea.

Conflict of interests The authors declare that there is no financial conflict of interests to publish these results.

References

1. Pellegrini M, Mansouri A, Simeone A, Boncinelli E, Gruss P. Dentate gyrus formation requires Emx2. Development 1996; 122(12): 3893-3898.
2. Bayer SA. Development of the hippocampal region in the rat. II. Morphogenesis during embryonic and early postnatal life. J Comp Neurol 1980; 190(1): 115-134.
3. Schlessinger AR, Cowan WM, Gottlieb DI. An autoradiographic study of the time of origin and the pattern of granule cell migration in the dentate gyrus of the rat. J Comp Neurol 1975; 159(2): 149-175.
4. Ngwenya LB, Heyworth NC, Shwe Y, Moore TL, Rosene DL. Age-related changes in dentate gyrus cell numbers, neurogenesis, and associations with cognitive impairments in the rhesus monkey. Front Syst Neurosci 2015; 9: 102.
5. Ortega-Martínez S. A new perspective on the role of the CREB family of transcription factors in memory consolidation via adult hippocampal neurogenesis. Front Mol Neurosci 2015; 8: 46.
6. Siegel GJ, Agranoff BW, Wayne Albers R, Fisher SK, Uhler MD. Basic Neurochemistry: Molecular, Cellular and Medical Aspects. Lippincott-Raven, Philadelphia, 2005; pp 637-670.
7. Simpson IA, Dwyer D, Malide D, Moley KH, Travis A, Vannucci SJ. The facilitative glucose transporter GLUT3: 20 years of distinction. Am J Physiol Endocrinol Metab 2008; 295(2): E242-253.
8. Vannucci SJ, Maher F, Simpson IA. Glucose transporter proteins in brain: delivery of glucose to neurons and glia. Glia 1997; 21(1): 2-21.
9. Guo X, Geng M, Du G. Glucose transporter 1, distribution in the brain and in neural disorders: its relationship with transport of neuroactive drugs through the blood-brain barrier. Biochem Genet 2005; 43(3-4): 175-187.
10. Maher F, Vannucci SJ, Simpson IA. Glucose transporter proteins in brain. FASEB J 1994; 8(13): 1003-1011.

11. Nehlig A, de Vasconcelos AP, Boyet S. Quantitative autoradiographic measurement of local cerebral glucose utilization in freely moving rats during postnatal development. J Neurosci 1988; 8(7): 2321-2333.
12. Vannucci RC, Christensen MA, Stein DT. Regional cerebral glucose utilization in the immature rat: effect of hypoxia-ischemia. Pediatr Res 1989; 26(3): 208-214.
13. Altman J, Das GD. Autoradiographic and histological evidence of postnatal hippocampal neurogenesis in rats. J Comp Neurol 1965; 124(3): 319-335.
14. Bayer SA, Altman J. Hippocampal development in the rat: cytogenesis and morphogenesis examined with autoradiography and low-level X-irradiation. J Comp Neurol 1974; 158(1): 55-79.
15. Yoo DY, Yoo KY, Park JH, Choi JW, Kim W, Hwang IK, Won MH. Detailed differentiation of calbindin d-28k-immunoreactive cells in the dentate gyrus in C57BL/6 mice at early postnatal stages. Lab Anim Res 2011; 27(2): 153-159.
16. Hebel R, Stromberg MW. Anatomy and Embryology of the Laboratory Rat. BioMed Verlag, W örthsee, 1986.
17. Vannucci SJ. Developmental expression of GLUT1 and GLUT3 glucose transporters in rat brain. J Neurochem 1994; 62(1): 240-246.
18. Aghajanian GK, Bloom FE. The formation of synaptic junctions in developing rat brain: a quantitative electron microscopic study. Brain Res 1967; 6(4): 716-727.
19. Ghosh A, Greenberg ME. Calcium signaling in neurons: molecular mechanisms and cellular consequences. Science 1995; 268(5208): 239-247.
20. Riccio A, Ahn S, Davenport CM, Blendy JA, Ginty DD. Mediation by a CREB family transcription factor of NGF-dependent survival of sympathetic neurons. Science 1999; 286(5448): 2358-2361.
21. Jin N, Qian W, Yin X, Zhang L, Iqbal K, Grundke-Iqbal I, Gong CX, Liu F. CREB regulates the expression of neuronal glucose transporter 3: a possible mechanism related to impaired brain glucose uptake in Alzheimer's disease. Nucleic Acids Res 2013; 41(5): 3240-3256.
22. Rajakumar A, Thamotharan S, Raychaudhuri N, Menon RK, Devaskar SU. Trans-activators regulating neuronal glucose transporter isoform-3 gene expression in mammalian neurons. J Biol Chem 2004; 279(25): 26768-26779.
23. Rajakumar RA1, Thamotharan S, Menon RK, Devaskar SU. Sp1 and Sp3 regulate transcriptional activity of the facilitative glucose transporter isoform-3 gene in mammalian neuroblasts and trophoblasts. J Biol Chem 1998; 273(42): 27474-27483.
24. Reddy AB, Srivastava SK, Ramana KV. Aldose reductase inhibition prevents lipopolysaccharide-induced glucose uptake and glucose transporter 3 expression in RAW264.7 macrophages. Int J Biochem Cell Biol 2010; 42(6): 1039-1045.
25. Hwang IK, Yoo KY, Yoo DY, Choi JW, Lee CH, Choi JH, Yoon YS, Won MH. Time-course of changes in phosphorylated CREB in neuroblasts and BDNF in the mouse dentate gyrus at early postnatal stages. Cell Mol Neurobiol 2011; 31(5): 669-674.